

## REVIEW OF b-FLAVORED HADRON SPECTROSCOPY

G. Eigen

*Department of Physics, University of Bergen, Allegaten 55, 5007 Bergen, Norway*

The current status of b-flavored hadron spectroscopy is reviewed.

### 1 Introduction

B-flavored hadrons are the heaviest flavored hadrons, since due to  $V_{tb} \sim 1$  the top quark decays long before forming bound states. They are copiously produced in  $p\bar{p}$  collisions at the Tevatron and in  $Z^0$  decays at LEP. Each LEP experiment has collected  $8.8 \times 10^5$   $b\bar{b}$  events. The formation of B-mesons versus b-baryons at the  $Z^0$  is favored by 9:1. The heavy quark ( $\bar{Q}$ ) also dresses favorably with light quarks produced in soft gluon processes. This leads to production rates of  $B_u^+ : B_d^0 : B_s^0 = 1 : 1 : \frac{1}{3}$ .  $B_c$  production is reduced by 2 – 3 orders of magnitude, since a hard gluon process is needed.

The properties of heavy-light systems ( $\bar{Q}q$  or  $Qqq$ ) are predicted by heavy quark effective theory (HQET),<sup>39</sup> which is based on the observation that in the limit  $m_Q \rightarrow \infty$  the heavy quark decouples from the light degrees of freedom. The heavy quark symmetry provides a good approximation for b hadrons since  $m_b \gg \Lambda_{QCD}$  and corrections obtained from a  $\frac{1}{m_b}$  expansion are small. In the heavy quark limit, also the spin of the heavy quark,  $s_Q$ , decouples from the orbital angular momentum of the system,  $l$ , and the spin of the light quark(s)  $s_q$ . Both  $s_Q$  and  $j = l \oplus s_q$  are separately conserved. Thus, states are grouped into doublets bearing similar properties. The  $B$  and  $B^*$  belong to the same doublet. The  $l = 1$  orbital excitations, frequently called  $B^{**}$ 's, fall into two doublets. The  $j = \frac{1}{2}$  states which include the scalar  $B_0^*$  and the axial vector  $B_1^*$  are broad decaying dominantly via S-wave to  $B\pi$  and  $B^*\pi$ , respectively. The  $j = \frac{3}{2}$  states which include the axial vector  $B_1$  and the tensor  $B_2^*$  are narrow. Their dominant decays proceed via D-wave to  $B^*\pi$  and  $B^{(*)}\pi$ , respectively. At the  $Z^0$  the production of  $l = 0$  B-mesons versus  $l = 1$  B-mesons is favored by 7:3. According to spin counting 75% of the  $l = 0$  B-states are  $B^*$ 's. The  $B^{**}$ 's decay strongly to  $B^*$ 's or  $B$ 's with a ratio ranging between 1 : 1 and 3 : 1. Thus, B-mesons are the best laboratory to test HQET predictions.

The crucial experimental tool for b-hadron spectroscopy is inclusive b hadron reconstruction. For  $b\bar{b}$  events selected via impact parameter tagging or via high  $p_t$  muons, energy and momentum of the b-hadron are reconstructed, using either a rapidity algorithm (ALEPH,<sup>2</sup> DELPHI<sup>3</sup>) or secondary vertex

reconstruction (OPAL<sup>4</sup>). For events consistent with a b-hadron the Q-value defined by  $Q_{BX} = m_{BX} - m_B - m_X$  is determined. For the majority of events in the final sample DELPHI<sup>3</sup> e.g. achieves an energy resolution of  $\sigma_E/E = 7\%$  and angular resolutions of  $\sigma_\phi \simeq \sigma_\theta \simeq 15$  mr.

## 2 Status of Pseudoscalar and Vector B Mesons

The  $B^+$  and  $B^0$  masses have been measured rather precisely by CLEO<sup>5</sup> ARGUS<sup>6</sup> and CDF.<sup>7</sup> The fits performed by the PDG<sup>8</sup> yield:  $m_{B^+} = 5278.9 \pm 1.8$  MeV and  $m_{B_d^0} = 5279.2 \pm 1.8$  MeV. The errors are dominated by a systematic uncertainty in determining the  $e^+e^-$  energy scale.<sup>5,6</sup> The  $B^0$  is heavier than the  $B^+$  as expected. However, the observed mass difference of  $m_{B_d^0} - m_{B^+} = 0.35 \pm 0.29$  is consistent with zero. The  $B_s^0$  mass has been measured rather precisely by CDF<sup>7</sup> in the  $B_s^0 \rightarrow J/\psi\phi$  channel (see Figure 1). The present  $B_s^0$  mass measurements are depicted in Figure 2. Including the LEP results<sup>9,10,11</sup> the PDG mass fit yields  $m_{B_s^0} = 5369.3 \pm 2.0$  MeV. This constrains the  $B_s^0 - B_d^0$  mass splitting to  $90 \pm 2.7$  MeV which is consistent with a quenched lattice QCD prediction of  $107 \pm 13$  MeV.<sup>12</sup> The  $B_c$  meson is not yet observed. Searches have been conducted by all four LEP experiments<sup>13,14,15,16</sup> and by CDF.<sup>17</sup> The channels studied include  $J/\psi\pi^+$ ,  $J/\psi a_1^+$  and  $J/\psi l\nu_l$ . Individual candidates are seen but are consistent with the expected background. The most serious candidate is reported by ALEPH<sup>13</sup> in the  $J/\psi\mu\nu_\mu$  channel and has a mass of  $m = 5.96 \pm 0.25 \pm 0.19$  GeV.

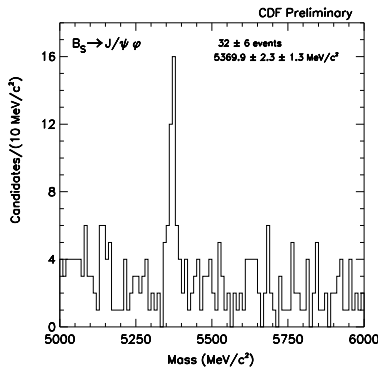


Figure 1. The  $J/\psi\phi$  invariant mass spectrum observed by CDF.

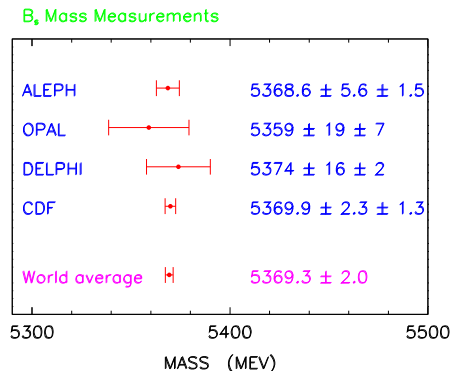


Figure 2. Summary of all  $B_s^0$  mass measurements.

In the heavy quark expansion hyperfine splittings (HFS) are proportional to  $\frac{1}{m_Q}$ . Thus, the  $B$  and  $B^*$  are much closer spaced than the  $D$  and  $D^*$ . A quenched lattice calculation e.g. yields  $\Delta m_B^{HFS} := m_{B_{u,d}^*} - m_{B_{u,d}} = 34 \pm 6$  MeV and  $\Delta m_{B_s}^{HFS} := m_{B_s^*} - m_{B_s} = 27 \pm 17$  MeV.<sup>12</sup> The small HFS permits only electromagnetic (EM) transitions, of which  $B^* \rightarrow \gamma B$  is the dominant one. For  $B^*$  reconstruction the low-energy photon needs to be detected. At LEP, however, the photon energy is boosted, maximally up to 800 MeV. L3 detects the photon directly in a crystal calorimeter, whereas the other LEP experiments reconstruct  $e^+e^-$  conversions. Typical energy and angular resolutions are  $\sigma_E/E = 1 - 2\%$  and  $\sigma_{\theta,\phi} = 1 - 2$  *mr*, respectively.

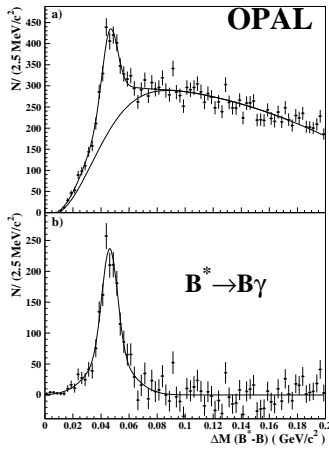


Figure 3. The  $B^* - B$  HFS observed by OPAL.

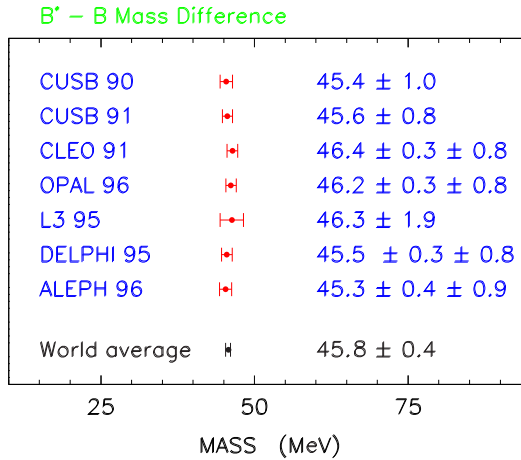


Figure 4. Summary of all  $B^* - B$  HFS measurements.

Figure 3 shows the  $Q_{B\gamma}$ -value distribution measured by OPAL.<sup>18</sup> Since the B-meson flavor is not identified,  $\Delta m_B^{HFS}$  includes contributions from  $B^+$ ,  $B_d^0$  and  $B_s^0$ . Figure 4 summarizes all  $\Delta m_B^{HFS}$  measurements from LEP<sup>18,19,20,21</sup> plus some old results from CLEO II<sup>22</sup> and CUSB.<sup>23</sup> The world average of the  $B^* - B$  hyperfine splitting is  $\Delta m_B^{HFS} = 45.79 \pm 0.35$  MeV. DELPHI<sup>20</sup> also has set 95% CL limits on  $B^+ - B_d^0$  and  $B_{u,d}^+ - B_s^0$  HFS differences, yielding:  $|\Delta m_{B_u}^{HFS} - \Delta m_{B_d}^{HFS}| < 6$  MeV and  $|\Delta m_{B_s}^{HFS} - \Delta m_{B_{u,d}}^{HFS}| < 6$  MeV.

All LEP experiments have measured the relative  $B^*$  production cross sec-

tion in  $Z^0$  decays.<sup>18,19,20,21</sup> Ignoring feed-down from  $B^{**}$ 's the LEP average is  $\frac{\sigma_{B^*}}{\sigma_B + \sigma_{B^*}} = 0.748 \pm 0.004$ . This agrees with expectations from naive spin counting, since the adjustment due to feed-down from  $B^{**}$ 's is only a few % effect depending on assumptions made for  $B^{**}$  decays. ALEPH,<sup>19</sup> DELPHI<sup>20</sup> and OPAL<sup>18</sup> also have measured the  $B^*$  polarization. The observed helicity angle distribution is uniform, indicating that all helicity states are equally populated. The combined LEP result for the longitudinal helicity component is  $\frac{\sigma_L}{\sigma_T + \sigma_L} = 0.33 \pm 0.04$ .

Though the M1 transition is nearly 100%, higher order EM transitions like the  $B^*$  Dalitz decays should also occur. The branching fraction independent of a form factor model is expected to be  $B(B^* \rightarrow Be^+e^-) \simeq 0.466\%$ .<sup>24</sup> Since the  $e^+$  and  $e^-$  momenta are below 100 MeV, electron identification and tracking in the vertex detector are essential. DELPHI has combined Dalitz pairs originating from the primary vertex with a B candidate.<sup>25</sup> The resulting  $Q_{Be^+e^-}$  distribution plotted in Figure 5 shows a peak at the expected  $\Delta m_B^{HFS}$  value. The  $B^*$  Dalitz decay rate normalized to that of the M1 transition is measured to be:  $\Gamma(B^* \rightarrow Be^+e^-)/\Gamma(B^* \rightarrow B\gamma) = (4.7 \pm 1.1 \pm 0.9) \times 10^{-3}$ .

### 3 Status of Orbitally-Excited B-Mesons

HQET predicts two narrow and two broad  $B^{**}$  states similarly as in the  $D^{**}$  system. Using the heavy quark expansion Eichten, Hill and Quigg determine the masses and total widths of the two  $j = \frac{3}{2}$   $B_{u,d}^{**}$  states to be  $m_{B_1} = 5759$  MeV,  $m_{B_2^*} = 5771$  MeV,  $\Gamma_{B_1} = 21$  MeV and  $\Gamma_{B_2^*} = 25$  MeV, respectively.<sup>26</sup> A recent calculation by Falk and Mehen based on the heavy flavor expansion yields masses of  $m_{B_1} = 5780$  MeV and  $m_{B_2^*} = 5794$  MeV.<sup>27</sup> The masses of the  $j = \frac{1}{2}$  states are expected to lie about 100 MeV lower than those of the  $j = \frac{3}{2}$  states.

ALEPH,<sup>29</sup> DELPHI<sup>30,31</sup> and OPAL<sup>32</sup> have analyzed single  $\pi^+$  transitions using inclusive B reconstruction methods. The Q-value distribution measured by DELPHI is plotted in Figure 6. A broad structure is observed at  $m = 5734 \pm 5 \pm 17$  MeV. A decomposition into individual  $j = \frac{3}{2}$  and  $j = \frac{1}{2}$  states is presently not conclusive. Similar observations have been found by the other LEP experiments. A summary of all mass measurements is shown in Figure 7. Note that the masses from OPAL and ALEPH shown here have been shifted up by 31 MeV<sup>a</sup> to account for dominant contributions from  $B^*\pi$  transitions.<sup>31</sup> The combined LEP result for the  $B_{u,d}^{**}$  mass is  $m(B_{u,d}^{**}) = 5722 \pm 8$  MeV. This is lower than the mass predictions for  $j = \frac{3}{2}$  states, thus leaving room

<sup>a</sup>We have assumed that  $B^*\pi$  versus  $B\pi$  transitions are enhanced by  $2 \pm 1 : 1$ , by considering various scenarios for  $B^{**}$  production and decay.<sup>33</sup>

for contributions from the  $j = \frac{1}{2}$  states. ALEPH, in addition, has performed an exclusive analysis in the  $B\pi$  channel.<sup>34</sup> A significant narrow structure is seen at  $m = 5703 \pm 14$  MeV. The resolution of  $\sigma = 28 \pm_{14}^{18}$  MeV would permit contributions from both  $j = \frac{3}{2}$  states. However, even after the +31 MeV shift,<sup>33</sup> the mass is still too low to agree with a DELPHI measurement obtained in the  $B^{(*)}\pi\pi$  final state (see below).

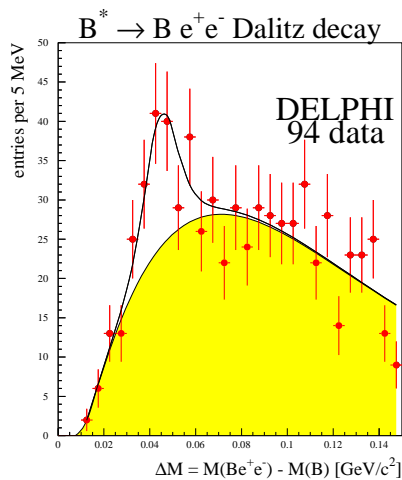


Figure 5. The  $Q$ -value distribution for  $B^*$  Dalitz decays.

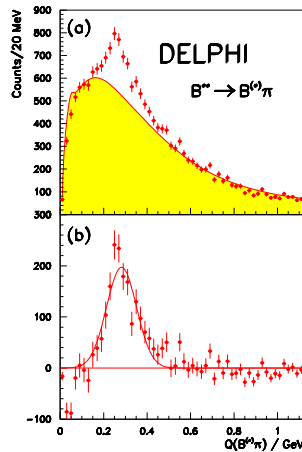


Figure 6. The  $Q$ -value distribution for  $B^{(*)}\pi$  final states.

The decay angle distribution of the  $\pi$  in the  $B^{**}$  rest frame provides information on the helicity distribution of the light quark system.<sup>28</sup> DELPHI has observed a uniform decay angle distribution,<sup>30</sup> which implies that the maximally allowed helicity components of the light quark system are not suppressed. This is surprising since ARGUS has observed the opposite for  $D_2^*$  decays.<sup>35</sup> Assuming that the contribution of decays from the  $j = \frac{1}{2}$  states, which produce a non-uniform decay angle distribution, is small, a fraction of  $w_{\frac{3}{2}} = 0.53 \pm 0.07 \pm 0.10$  is measured for the helicity  $j = \pm \frac{3}{2}$  components.<sup>b</sup>

The masses predicted by Eichten, Hill and Quigg for the narrow  $B_s^{**}$  states are  $m_{B_{s1}} = 5849$  MeV and  $m_{B_{s2}} = 5861$  MeV.<sup>26</sup> Predictions by Falk and Mehen

<sup>b</sup>The S-wave decays  $B_0^* \rightarrow B\pi$  and  $B_1^* \rightarrow B^*\pi$  are expected to be dominant.

are again higher, yielding  $m_{B_{s1}} = 5886$  MeV and  $m_{B_{s2}^*} = 5899$  MeV.<sup>27</sup> Since the  $B_s^{**} - B_{u,d}$  mass difference is larger than the kaon mass, the dominant transitions are  $B_s^{**} \rightarrow KB_{u,d}^*$ .

Using the inclusive analysis techniques DELPHI has studied  $B^{(*)}K^\pm$  final states.<sup>31</sup> DELPHI is rather suited for analyzing such channels because of their excellent kaon identification over a wide momentum range.<sup>36</sup> The resulting  $Q$ -value distribution depicted in Figure 8 shows two narrow structures at  $70 \pm 4 \pm 8$  MeV and  $142 \pm 4 \pm 8$  MeV. Their widths are slightly smaller than the observed resolution. Assuming that the upper peak stems from the transition  $B_{s1} \rightarrow B^*K$  and the lower peak stems from  $B_{s2}^* \rightarrow BK$ , masses of  $m_{B_{s1}} = 5888 \pm 4 \pm 8$  MeV and  $m_{B_{s2}^*} = 5914 \pm 4 \pm 8$  MeV have been obtained. The mass splitting is  $m_{B_{s2}^*} - m_{B_{s1}} = 26 \pm 6 \pm 8$  MeV. Both the masses and the splitting are higher than the HQET predictions. In addition, upper limits have been set on the widths, yielding  $\Gamma_{B_{s1}} < 60$  MeV and  $\Gamma_{B_{s2}^*} < 50$  MeV at 95% CL, respectively. The production cross sections for  $B_{s1}$  and  $B_{s2}^*$  states with respect to that of  $B_{u,d}^{**}$  has been measured to be:  $(\sigma_{B_{s1}} + \sigma_{B_{s2}^*})/\sigma_{B_{u,d}^{**}} = 0.142 \pm 0.028 \pm 0.047$ . OPAL<sup>32</sup> has also studied this channel, observing a  $\Gamma = 47$  MeV broad structure at  $m = 5853 \pm 15$  MeV, which again needs to be shifted upward by  $\sim 31$  MeV to account for dominant  $B^*K$  transitions.

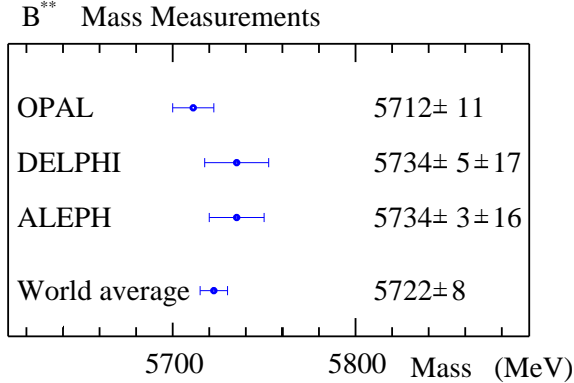


Figure 7. Summary of all inclusive  $B^{**}$  mass measurements.

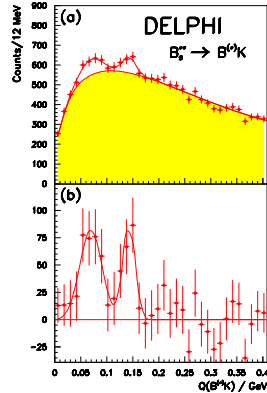


Figure 8. The  $Q$ -value distribution for  $BK^\pm$  final states.

## 4 First Observation of Radially Excited B Mesons

Radial excitations of D mesons and B mesons should exist similarly as those of  $c\bar{c}$  and  $b\bar{b}$  states.<sup>39</sup> A QCD inspired relativistic quark model predicts the masses of the 2S pseudoscalar and vector states to lie at 5900 MeV and 5930 MeV, respectively.<sup>40</sup> DELPHI has extended the inclusive analysis to  $\pi^+\pi^-$  transitions to look for such states.<sup>37,38</sup> For  $b\bar{b}$  events with a  $\pi^+\pi^-$  pair from the primary vertex where both pions have large rapidities ( $\eta > 2.5$ ) and are in the same hemisphere as the B candidate, the variable,  $Q_{B\pi\pi} = m_{B^{(*)}\pi^+\pi^-} - m_{B^{(*)}} - 2m_{\pi^\pm}$ , was determined. This selection is  $52 \pm 3\%$  efficient and has a purity of  $80 \pm 4\%$ . The resulting Q-value distribution displayed in Figure 9 shows two narrow structures, one at  $Q_{B^{(*)}\pi\pi} = 301 \pm 4 \pm 10$  MeV containing  $56 \pm 13$  events and a second at  $Q_{B^{(*)}\pi\pi} = 220 \pm 4 \pm 10$  MeV containing  $60 \pm 12$  events. The corresponding measured resolutions,  $\sigma = 12 \pm 3$  MeV and  $\sigma = 15 \pm 3$  MeV, are compatible with the detector resolution, implying that their natural widths must be narrow. Thus, the two broad  $j = \frac{1}{2}$  orbital excitations cannot contribute significantly here.

Figure 10 shows all allowed transitions for the 2S states and 1P states. The non-suppressed  $\pi$  and  $\pi\pi$  transitions of the narrow  $j = 3/2$  P states are:  $B_1 \rightarrow B^* \pi$  (D-wave),  $B_1 \rightarrow B \pi\pi$  &  $B_1 \rightarrow B^* \pi\pi$  (P-wave);  $B_2^* \rightarrow B\pi$  &  $B_2^* \rightarrow B^* \pi$  (D-wave), and  $B_2^* \rightarrow B^* \pi\pi$  (P-wave). The corresponding transitions of the 2S states are:  $B' \rightarrow B^* \pi$  (P-wave),  $B' \rightarrow B_0^* \pi$  &  $B' \rightarrow B\pi\pi$  (S-wave);  $B^{*'} \rightarrow B\pi$  &  $B^{*'} \rightarrow B^* \pi$  (P-wave), and  $B^{*'} \rightarrow B_1 \pi$  &  $B^{*'} \rightarrow B^* \pi\pi$  (S-wave).  $\rho$  transitions are suppressed by phase space. Since the mass resolution is smaller than  $\Delta m_B^{HFS}$ , we can exclude that a single excited state decays to  $B\pi\pi$  and  $B^* \pi\pi$  simultaneously. In that case two peaks separated by  $\Delta m_B^{HFS}$  should have been visible. It is, however, possible that the two peaks originate from two closely spaced excited states, where the heavier decays to  $B^* \pi\pi$  and the lighter to  $B\pi\pi$ .

The lower peak most likely stems from the P-wave transitions,  $B_1 \rightarrow B\pi^+\pi^-$  with a possible contribution from  $B_2^* \rightarrow \pi^+\pi^- B^*$ . Denoting the mass splitting of the  $j = \frac{3}{2}$  states by  $\Delta m_{B_{3/2}} := m_{B_2^*} - m_{B_1}$  and the fraction of  $B_2^*$  decays by  $f$ , we can parametrize the masses of the narrow states by:  $m_{B_1} = 5778 + f \cdot (\Delta m_B^{HFS} - \Delta m_{B_{3/2}}) \pm 11$  MeV and  $m_{B_2^*} = 5824 - (1 - f) \cdot (\Delta m_B^{HFS} - \Delta m_{B_{3/2}}) \pm 11$  MeV. These mass estimates are consistent with the heavy quark predictions for  $j = \frac{3}{2}$  states, but they are higher than the mass of the broad structure observed in Figure 6. This implies that  $j = \frac{1}{2}$  states contribute significantly there. Assuming that  $0 \leq \Delta m_{B_{3/2}} \leq \Delta m_B^{HFS}$  as in the D-system, we can set bounds of  $m_{B_1} > 5756$  MeV and  $m_{B_2^*} < 5846$  MeV @95% CL, which are in conflict with the exclusive  $B^{(*)}\pi$  ALEPH result.<sup>34</sup>

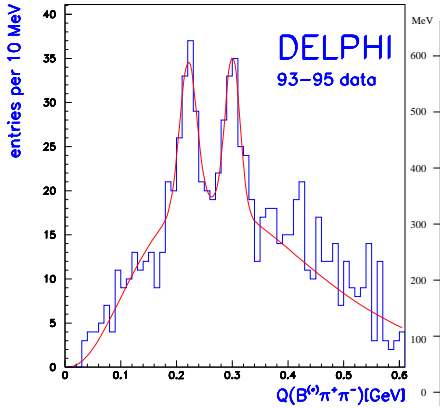


Figure 9. The  $Q$ -value distribution for  $B^{(*)}\pi^{\pm}\pi^{\mp}$  final states.

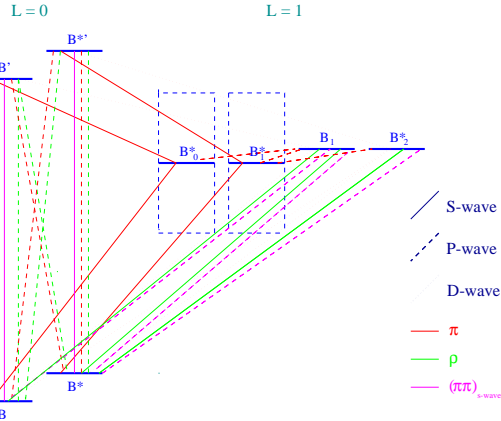


Figure 10.  $B$ -meson level diagram with expected hadronic transitions.

The upper peak has to originate from states which lie  $\geq 80$  MeV above the  $B_1$ . The most likely interpretation is that this peak stems from  $\pi\pi$  transitions of the 2S radial excitations:  $B' \rightarrow B\pi\pi$  and  $B^{*'} \rightarrow B^*\pi\pi$ . The S-wave  $\pi\pi$  transitions are expected to be dominant, though two successive  $\pi$  transition via the broad  $j = \frac{1}{2}$  orbital excitations are kinematically allowed. However, more detailed studies are needed to clarify this issue. Though single  $\pi$  transitions  $B^{(*)'} \rightarrow B^{(*)}\pi$  are allowed, they should be suppressed because of nodes in the radial wave functions, which lead to cancellations in the overlap integral.<sup>40</sup> Such cancellations have been observed in  $\rho' \rightarrow \pi\pi$ <sup>41</sup> and  $\psi(4040) \rightarrow D\bar{D}$ <sup>42</sup> decays. Nevertheless, the observed  $Q$ -value distribution for  $B^{(*)}\pi$  final states actually has room for such transitions. Assuming that the production of  $B^{*'}$  to  $B'$  is similar to that of  $B^*$  to  $B$ , we obtain the following mass estimates for the 2S states:  $m_{B'} = 5859 + \frac{3}{4}(\Delta m_B^{HFS} - \Delta m_{B'}^{HFS}) \pm 12$  MeV and  $m_{B^{*'}} = 5905 - \frac{1}{4}(\Delta m_B^{HFS} - \Delta m_{B'}^{HFS}) \pm 12$  MeV. Here  $\Delta m_B^{HFS}$  denotes the HFS of the radially excited states. These values are consistent with predictions from a QCD inspired relativistic quark model, thus supporting the interpretation of observing 2S radial excitations.<sup>40</sup> A preliminary estimate of the production cross sections from the observed signal yield is:  $\sigma(b \rightarrow B' + B^{*'})/\sigma(b \rightarrow all) = 0.5\% - 4\%$ . The branching ratio for  $B_1 \rightarrow B\pi\pi$  is of the order of 2% - 10%.

## 5 Status of b Baryons

The  $\Lambda_b$  is clearly established since a recent CDF measurement in the  $\Lambda J/\psi$  channel.<sup>43</sup> The  $\Lambda J/\psi$  invariant mass peaks at  $m_{\Lambda_b} = 5621 \pm 4 \pm 3$  MeV. Previously, ALEPH<sup>44</sup> and DELPHI<sup>45</sup> had observed a few candidates in the  $\Lambda_c^\pm \pi^\mp$  channel. All mass measurements are summarized in Figure 11. The present world average for the  $\Lambda_b$  mass is  $m_{\Lambda_b} = 5624 \pm 9$  MeV.<sup>8</sup>

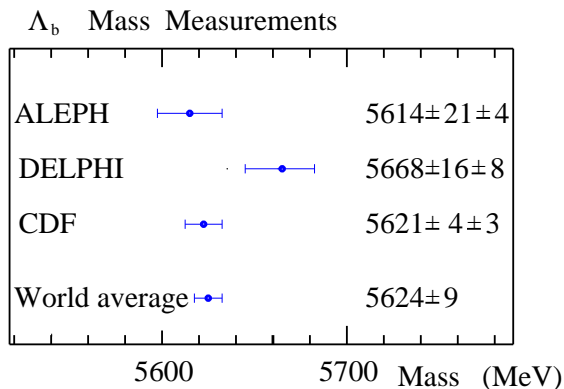


Figure 11. Summary of  $\Lambda_b$  mass measurements.

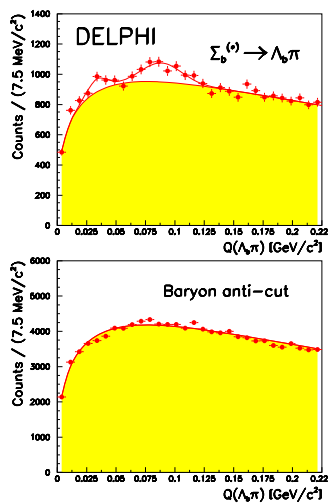


Figure 12. The  $Q$ -value distribution for  $\Lambda_b \pi$  final states.

Using the heavy quark expansion in combination with the observed  $\Sigma_c^* - \Sigma_c$  HFS provides a prediction for the  $\Sigma_b^* - \Sigma_b$  HFS of  $\Delta m_{\Sigma_b}^{HFS} = 22$  MeV.<sup>46</sup> DELPHI<sup>47</sup> has looked for b-flavored baryons using the inclusive analysis techniques. Baryon enrichment is obtained by selecting fast p's, n's and  $\Lambda$ 's. For events consistent with a  $\Lambda_b$ , a pion from the primary vertex is added to determine the variable  $Q_{\Lambda_b \pi} = m_{\Lambda_b \pi} - m_{\Lambda_b} - m_\pi$ . The resulting distribution depicted in Figure 12 reveals two structures at  $Q_{\Lambda_b \pi} = 33 \pm 3 \pm 8$  MeV and  $Q_{\Lambda_b \pi} = 89 \pm 3 \pm 8$  MeV. Interpreting these as transitions from the  $\Sigma_b$  and  $\Sigma_b^*$ , mass differences of  $m_{\Sigma_b} - m_{\Lambda_b} = 173 \pm 3 \pm 8$  MeV and  $m_{\Sigma_b^*} - m_{\Lambda_b} = 229 \pm 3 \pm 8$  MeV are determined. Within errors they are consistent with quark model predictions<sup>48</sup> yielding  $m_{\Sigma_b} - m_{\Lambda_b} = 200 \pm 20$  MeV and  $m_{\Sigma_b^*} - m_{\Lambda_b} = 230 \pm 20$  MeV,



## 6 Summary

The knowledge of the B meson sector has improved over the past few years. The present status is summarized in Figure 13. Precisely measured masses exist for all pseudoscalar and vector B meson ground states except for those in the  $B_c$  system, which has not been detected yet. Evidence is found for orbital excitations, but only in the  $B_s^0$  system it was possible to isolate two separate narrow states. Cross section measurements agree with expectations and decay angle distributions indicate that helicity  $j = \pm\frac{3}{2}$  states are not suppressed. While presently there is no evidence for orbital excitations with  $L > 1$ , first evidence is found for the  $2S$   $B_{u,d}$  radial excitations.

States and transitions in the b-baryon sector are summarized in Figure 14. The knowledge is still rather poor here. Only the  $\Lambda_b$  is well-established. The  $\Sigma_b$  and  $\Sigma_b^*$  may be observed but the HFS is in conflict with HQET predictions. Thus, these measurements need confirmation. The mass of the  $\Xi_b$  is unknown, though its lifetime has been measured.<sup>8</sup> So far no other b-flavored baryon has been identified.

## 7 Acknowledgments

This work has been supported by the Research Council of Norway. I would like to acknowledge the DELPHI collaboration for support. Special thanks goes to M. Feindt, Ch. Weiser and Ch. Kreuter for fruitful discussions.

## References

1. N. Isgur and M.Wise, *Phys. Lett. B* **232**, 113 (1989); *Phys. Lett. B* **237**, 527 (1990).
2. D. Buskulic et al., *Phys. Lett. B* **313**, 535 (1993).
3. P.Abreu et al., *Z. Phys. C* **68**, 353 (1995); *Phys. Lett. B* **345**, 598 (1995)
4. G. Alexander et al., *Z. Phys. C* **66**, 19 (1995).
5. S. Alam et al., *Phys. Rev. D* **50**, 43 (1994); Bortoletto et al., *Phys. Rev. Lett.* **64**, 2117 (1990) .
6. H. Albrecht et al., *Phys. Lett. B* **335**, 526 (1994).
7. F. Abe et al., *Phys. Rev. D* **53**, 3496 (1996).
8. R.M. Barnett et al., *Phys. Rev. D* **54**, 1 (1996).
9. D. Buskulic et al., *Z. Phys. C* **69**, 425 (1993).
10. P.Abreu et al., *Phys. Lett. B* **324**, 500 (1994).
11. R. Akers et al., *Phys. Lett. B* **337**, 196 (1994).
12. J.P. Ma and B.H.J. McKellar, UM-P-97/26, RCHEP-97/04 (1997).
13. D. Barate et al., *Phys. Lett. B* **402**, 213 (1997).

14. P.Abreu et al., *Phys. Lett. B* **398**, 207 (1997).
15. M. Acciarri et al., ICHEP conf. Pa05-046, Warsaw (1996).
16. G. Alexander et al., *Z. Phys. C* **70**, 197 (1996).
17. F. Abe et al., *Phys. Rev. Lett.* **77**, 5176 (1996).
18. K. Akerstaff et al., *Z. Phys. C* **74**, 413 (1997).
19. D. Buskulic et al., *Z. Phys. C* **69**, 393 (1996).
20. P.Abreu et al., *Z. Phys. C* **68**, 353 (1995).
21. M. Acciarri et al., *Phys. Lett. B* **345**, 589 (1995).
22. D. Akerib et al., *Phys. Rev. Lett.* **67**, 1692 (1991).
23. J. Lee-Franzini et al., *Phys. Rev. Lett.* **65**, 2947 (1990); Q.W. Wu et al., *Phys. Lett. B* **273**, 177 (1991).
24. L.G. Landsberg, *Phys. Rep.* **128**, 301 (1985).
25. P.Abreu et al., DELPHI-96-93, ICHEP conf. Pa1-021, Warsaw (1996); DELPHI-97-99, EPS-0450 EPS conf. Jerusalem (1997).
26. E.J. Eichten, Ch.T. Hill and Ch. Quigg, *Phys. Rev. Lett.* **71**, 4116 (1993); Fermilab-Conf-94/118-T.
27. A.F. Falk and T. Mehen, *Phys. Rev. D* **53**, 231 (1996).
28. A.F. Falk and M. Peskin, *Phys. Rev. D* **49**, 3320 (1994).
29. D. Buskulic et al., *Z. Phys. C* **69**, 393 (1996).
30. P.Abreu et al., *Phys. Lett. B* **345**, 98 (1995).
31. P.Abreu et al., EPS-0563 Brussels EPS conf. Brussels (1995).
32. R. Akers et al., *Z. Phys. C* **66**, 19 (1995).
33. M. Feindt, private communication.
34. D. Buskulic et al., EPS-0403 EPS conf. Brussels (1995).
35. H.Albrecht et al., *Phys. Lett. B* **221**, 422 (1989).
36. P. Aariano et al., *Nucl. Instrum. Methods A* **303**, 233 (1991); P.Abreu et al., *Nucl. Instrum. Methods A* **378**, 57 (1996).
37. G. Eigen, *J. Mod Phys.A* **12**, 3909 (1997).
38. P.Abreu et al., ICHEP-96 PA01-021, Warsaw (1996).
39. S. Godfrey and N. Isgur, *Phys. Rev. D* **32**, 189 (1985).
40. R. Kokoski and N. Isgur, *Phys. Rev. D* **35**, 907 (1987).
41. W.B. Kaufmann, R.J. Jacob, *Phys. Rev. D* **10**, 1051 (1974).
42. A. Le Yaouanc et al., *Phys. Lett. B* **71**, 397 (1977).
43. F. Abe et al., *Phys. Rev. D* **55**, 1142 (1997).
44. D. Buskulic et al., *Phys. Lett. B* **380**, 442 (1996).
45. P.Abreu et al., *Phys. Lett. B* **374**, 351 (1996).
46. A.F. Falk, *Int.J.Mod.Phys.A* **12** (1997) 4079.
47. P.Abreu et al., DELPHI-95-107, EPS-0565 EPS conf. Brussels (1995).
48. R. Roncaglia et al., *Phys. Rev. Lett.* **51**, 1248 (1995).
49. D. Buskulic et al., EPS-0400 EPS conf. Brussel (1995).